If the texture has a rotational symmetry with respect to an axis of the sample, the texture is referred to as a fibre texture and the axis is referred to as the fibre axis. The sample orientation containing the symmetry axis is referred to as the fibre axis. The fibre texture is mostly observed in two types of materials: metal wires or rods formed by drawing or extrusion, and thin films formed by physical or chemical deposition. The fibre axis is the wire axis for a wire and normal to the sample surface for thin films. Fibre texture can also be artificially formed by rotating a sample about its normal. If the fibre axis is aligned to the S_3 direction, the pole-density distribution function becomes independent of the azimuthal angle β. For samples with fibre texture, or artificially formed fibre texture by rotating, the pole-density function is conveniently expressed as a function of a single variable, $g_{hkl}(\chi)$. Here, χ is the angle between the sample normal and pole direction.

$$\chi = 90^\circ - \alpha \text{ or } \chi = \cos^{-1}|h_3|. \tag{2.5.59}$$

The pole-density function for fibre texture can be expressed as a fibre plot. The fibre plot $g_{hkl}(\chi)$ can be calculated from the relative intensity of several peaks (He, 1992; He *et al.*, 1994) and artificial fibre texture can be achieved by sample spinning during data collection.

2.5.4.2.3. *Data-collection strategy*

Since a one-dimensional pole-density mapping is created from each 2D frame, it is important to lay out a data-collection strategy so as to have the optimum pole-figure coverage and minimum redundancy in data collection. The pole-figure coverage can be simulated from the diffraction 2θ angle, detector swing angle, detector distance, goniometer angles and scanning steps. When a large 2D detector is placed close to the sample, it is possible to collect a pole figure with a single φ scan. Fig. 2.5.20(a) shows an example of a scheme generated by a single φ scan of 5° steps with a detector 10.5 cm in diameter and D = 7 cm. The data collected with a single exposure at $\varphi = 0^\circ$ would generate a one-dimensional pole figure as shown in the curve marked by A and B. The pole figure can be generated by a full-circle rotation of 360°. The pole density at the centre represents the diffraction vector perpendicular to the sample surface. It is important to have the pole-density information in the centre region of the pole figure, especially for fibre texture. The pole-figure angle at the centre is $\alpha = 90^\circ$, and the best strategy is to put point A at the centre of pole figure. That is

$$h_3^A = \sin\theta\cos\psi\sin\omega - \cos\theta\sin\gamma_A\cos\psi\cos\omega - \cos\theta\cos\gamma_A\sin\psi = 1. \tag{2.5.60}$$

In some cases, a single φ scan is not enough to cover sufficient pole-figure angles because of a large detector distance or limited detector area, so it is necessary to collect a set of data with φ scans at several different sample tilt angles. Fig. 2.5.20(b) illustrates the data-collection scheme with a detector that is 10.5 cm in diameter and D = 10 cm for the (111) plane of a Cu thin film. In this case, each pole figure requires two φ scans at different sample orientations. The data-collection strategy should also be optimized for several crystallographic planes if all can be covered in a frame. The step size of the data-collection scan depends highly on the strength of the texture and the purpose of the texture measurements. For a weak texture, or quality control for metal parts, φ (or ω, or ψ) scan steps of 5° may be sufficient. For strong textures, such as thin films with epitaxial structure, scan steps of 1° or smaller may be necessary.

The effectiveness of two-dimensional data collection for a texture can be compared with that using a point detector with the data-collection strategy of the Cu thin film as an example. Fig. 2.5.20(c) shows the pole-figure data-collection strategy with a point detector. For the same pole-figure resolution, significantly more exposures are required with a point detector. Considering that several diffraction rings are measured simultaneously with a 2D detector, the pole-figure measurement is typically 10 to 100 times faster than with a point detector. Therefore, quantitative high-resolution pole-figure measurements are only practical with a 2D-XRD system (Bunge & Klein, 1996).

2.5.4.2.4. *Texture-data processing*

For a specific diffraction ring, 2θ is a constant or at least assumed to be constant for texture analysis, and the sample-orientation angles (ω, ψ, φ) for a frame are also constants. Therefore, the pole-density information is given by the diffraction-intensity distribution as a function of γ only, or $I = I(\gamma)$. Integration of the diffraction intensities in the 2θ direction converts 2D information into the function $I(\gamma)$.

Fig. 2.5.21(a) shows a 2D diffraction ring for texture analysis. The low and high background and diffraction-ring 2θ–γ range are defined by three boxes, noted as B_L, B_H and $I(\gamma)$, respectively. All three boxes have the same γ range from γ_1 to γ_2. The 2θ ranges for the diffraction ring, low background and high background should be determined based on the width of the 2θ peak and available background between adjacent peaks. Assuming a normal distribution, a 2θ range of 2 times the FWHM covers 98% of the intensity peak, and 3 times the FWHM covers more than 99.9%. The 2θ range should also be broad enough to cover the possible 2θ shifts caused by residual stresses in the sample. Fig. 2.5.21(b) is the 2θ profile integrated over the section $\Delta\gamma$ in Fig. 2.5.21(a). The background ranges on the low and high 2θ sides are given by $2\theta_{L1}$–$2\theta_{L2}$ and $2\theta_{H1}$–$2\theta_{H2}$, respectively. The 2θ-integrated diffraction intensities as a function of γ are plotted in Fig. 2.5.21(c). The background can be calculated and removed from the intensity values of the low and high backgrounds or ignored if the contribution of the background is very small.

2θ integration without a background correction can be

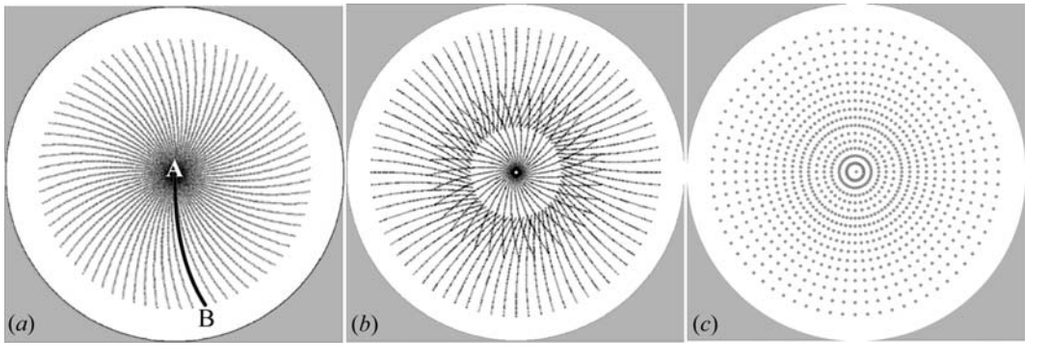

Figure 2.5.20
Data-collection strategy: (a) 2D detector with D = 7 cm; (b) 2D detector with D = 10 cm; (c) point detector.

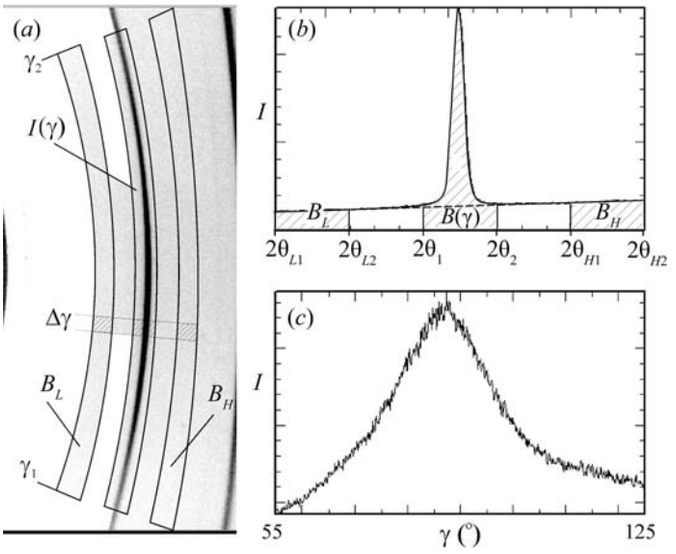

Figure 2.5.21
Pole-figure data processing: (*a*) a frame with the 2θ integration ranges for the (220) ring; (*b*) 2θ profile showing the background and peak; (*c*) integrated intensity distribution as a function of γ.

expressed as

$$I(\gamma) = \int_{2\theta_1}^{2\theta_2} J(2\theta, \gamma)\, \mathrm{d}(2\theta), \quad \gamma_1 \le \gamma \le \gamma_2. \tag{2.5.61}$$

A similar equation can be used for 2θ integration of the low and high backgrounds $B_L(\gamma)$ and $B_H(\gamma)$. Assuming a linear background change in the vicinity of the 2θ peak, the background under the peak, $B(\gamma)$, is then given by

$$B(\gamma) = B_L(\gamma)\frac{(2\theta_2 - 2\theta_1)(2\theta_{H2} + 2\theta_{H1} - 2\theta_2 - 2\theta_1)}{(2\theta_{L2} - 2\theta_{L1})(2\theta_{H2} + 2\theta_{H1} - 2\theta_{L2} - 2\theta_{L1})} + B_H(\gamma)\frac{(2\theta_2 - 2\theta_1)(2\theta_2 + 2\theta_1 - 2\theta_{L2} - 2\theta_{L1})}{(2\theta_{H2} - 2\theta_{H1})(2\theta_{H2} + 2\theta_{H1} - 2\theta_{L2} - 2\theta_{L1})}. \tag{2.5.62}$$

Then the background $B(\gamma)$ can be subtracted from the integrated intensity distribution $I(\gamma)$.

The algorithms of γ integration given in Section 2.5.4.2.3 can be easily modified for 2θ integration by exchanging γ and 2θ in the equations. Algorithms with solid-angle normalization should be used to get consistent integrated intensity over all areas of the detector. The 2θ-integrated intensity distribution can then be mapped onto a pole figure based on the fundamental equations (2.5.53) and (2.5.54). When a pole-figure pixel is overlapped by more than one data point from different scans, as shown in the region covered by two scans in Fig. 2.5.20(*b*), the average value should be mapped to that pole-figure pixel. Fig. 2.5.22(*a*) shows pole-density mappings on the pole figure. There are big gaps between the measured pole-density data points due to the large φ-scan steps of 5°.

All factors affecting relative intensities, such as Lorentz, polarization, air scattering, and Be-window and sample absorption, will have an effect on the measured pole densities for the pole figures. Some or all these corrections may be applied to the diffraction frames before 2θ integration if the texture study demands high accuracy in the relative pole densities. Among these factors, the most important factor is sample absorption, since data sets for pole figures are typically collected at several different incident angles. A ridge between the pole-density regions covered by two different incident angles may be observed if sample absorption is not properly corrected.

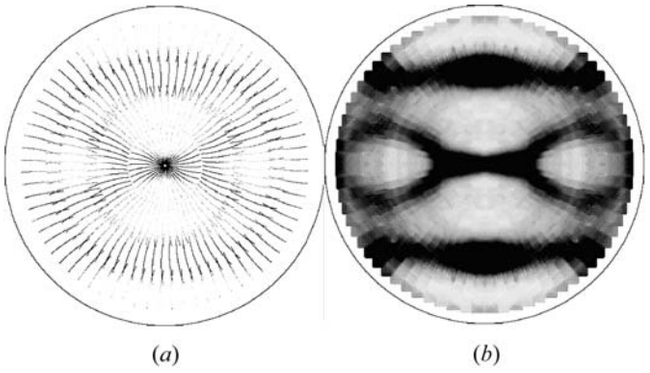

Figure 2.5.22
Pole-figure processing: (*a*) $I(\gamma)$ mapped to the pole figure; (*b*) Pole figure after interpolation and symmetry processing.

2.5.4.2.5. *Pole-figure interpolation and use of symmetry*

The pole figure is stored and displayed as a bitmap image. The pole-density data from the data set may not fill up all the pixels of the pole-figure image. In order to generate a smooth pole figure, the unmapped pixels are filled with values generated from the interpolation of the surrounding pixels. A linear interpolation within a defined box is sufficient to fill the unmapped pixels. The size of the box should be properly chosen. A box that is too small may not be able to fill all unmapped pixels and a box that is too big may have a smearing effect on the pole figure, especially if a sharp pole figure is processed. All the gaps between the measured pole-density points are filled after this interpolation. For a sample with sharp texture, smaller φ-scan steps should be used.

All pole figures possess symmetry as a consequence of the Laue symmetry of the crystallites in the sample. This symmetry can be used to fill in values for pixels in the pole figure for which data were not measured, or to smooth the pole figure. For example, orthorhombic materials exhibit *mmm* symmetry, thus one needs to collect only an octant or quadrant of the pole sphere to generate the entire pole figure. The pole figures of materials with higher symmetry may be treated by using lower symmetry in the processing. For instance, one can use 2/*m* or *mmm* symmetry for hexagonal materials and *mmm* for cubic materials. In symmetry processing, all the symmetry-equivalent pole-figure pixels are filled by the average value of the measured pixels. For the unmeasured pole-figure pixels, this symmetry processing fills in a value from the average of all the equivalent pixels. For the measured pixels, this average processing serves as a smoothing function. Fig. 2.5.22(*b*) shows the results after both interpolation and use of symmetry.

2.5.4.2.6. *Orientation relationship*

A 2D-XRD system can measure texture from a sample containing a single phase, multiple phases or single crystals. The orientation relationship between different phases, or thin films and substrates, can be revealed because data are collected from all phases of the sample simultaneously. One example is the measurement of pole figures for a magnetron sputter-deposited Cu film on an Si wafer (He *et al.*, 2005). Fig. 2.5.23 shows the overlapped pole figures of the Cu (111) film and Si (400) substrate in a 2D pole figure (*a*) and 3D surface plot (*b*). The three sharp spots from the (400) spots of the Si wafer show the wafer cut orientation of (111). The Cu (111) pole density maxi-